Journal of *Marine Science and Engineering*

MDPI

Article

Pullout Bearing Capacity of End-Bearing Torpedo Anchors in Cohesive Soil Seabed

Gang Li [1], Jinli Zhang [2,*], Jia Liu [3], Yu Xi [1] and Honggang Kou [1]

[1] Shaanxi Key Laboratory of Safety and Durability of Concrete Structures, Xijing University, Xi'an 710123, China; t_bag945@126.com (G.L.); xiyu@xijing.edu.cn (Y.X.); 20190020@xijing.edu.cn (H.K.)
[2] State Key Laboratory of Coastal and Offshore Engineering, Dalian University of Technology, Dalian 116024, China
[3] School of Geological Engineering and Geomatics, Chang'an University, Xi'an 710054, China; 15929935077@163.com
* Correspondence: jlzhang@dlut.edu.cn

Abstract: As a new type of deep-sea anchoring foundation, thetorpedo anchor has the characteristics of simple installation, low cost, and high bearing capacity. Compared with the torpedo anchor without an anchor wing, the end-bearing torpedo anchor forms pile end resistance using a bearing plate, thus further improving its uplift bearing capacity. By conducting the pullout model test of torpedo anchors, we have compared and analyzed the effects of the pullout angle and bearing-plate radius on the bearing characteristics of T, EN3, EN4, and EC types of torpedo anchors. Based on the model test results, we established the V-H envelope of torpedo-anchor bearing capacity using the regression analysis method. The results show that when the displacement is small, the load-displacement curve of the torpedo anchor increases in an approximately linear mode, and the curve fluctuates and gradually entersa stable state with the gradual increase of the displacement. With the increasing pullout angle, the bearing capacity of the torpedo anchor increases first and then decreases. When the pullout angle is 45°, the torpedo anchor has the maximum bearing capacity. When the pullout angle is constant, the order of bearing capacity generated by different types of torpedo anchors is as follows: EC > EN4 > EN3 > T, and the bearing capacity rises with the increasing bearing-plate area. Through regression analysis, it is concluded that for the torpedo anchors of T, EN3, EN4, and EC types, the V-H envelope of bearing capacity shows an outward convex trend, and the determination coefficient reaches 0.930, indicating that the established V-H envelope is suitable for predicting the bearing capacity of torpedo anchors.

Keywords: end-bearing; torpedo anchor; bearing capacity; pullout angle; cohesive soil

Citation: Li, G.; Zhang, J.; Liu, J.; Xi, Y.; Kou, H. Pullout Bearing Capacity of End-Bearing Torpedo Anchors in Cohesive Soil Seabed. *J. Mar. Sci. Eng.* **2023**, *11*, 1548. https://doi.org/10.3390/jmse11081548

Academic Editor: Erkan Oterkus

Received: 16 July 2023
Revised: 28 July 2023
Accepted: 2 August 2023
Published: 4 August 2023

1. Introduction

With the exhaustion of offshore oil and gas resources, the exploitation of oil and gas has gradually advanced from offshore areas to the deep sea, and the traditional mooring system cannot meet the needs therefrom [1–9]. As a new type of deep-sea anchoring foundation, the torpedo anchor takes the shape of the cylinder as a whole; the conical anchor tip is 30°, the interior is filled with concrete or scrap metal, and its weight is about 100 t. During installation, the torpedo anchor falls freely to obtain kinetic energy and then penetrates the seabed at the water depth of 30 to 150 m, thereby ensuring a sufficient penetration depth and obtaining a higher bearing capacity. The torpedo anchor has the advantages of simple installation, low cost, and high bearing capacity. Therefore, this type of anchor has attracted great attention fromacademia and the engineering industry [10]. Yu et al. [11,12] concluded that the uplift bearing capacity of the torpedo anchor with four anchor wings is 1.9 times greater than that of the torpedo anchor without an anchor wing, and the uplift bearing capacity is larger when the pullout-load angle is between 30° and 45°. When the anchor wing has the same lateral area, increasing the width of the anchor wing can effectively

improve the bearing capacity. When the length of the anchor wing is greater than 1/2 of the anchor length, the bearing capacity obtained by increasing the anchor wing width is higher than that obtained by increasing the anchor wing length. The research findings can provide a reference for the optimization design of torpedo anchors. Based on the sediment rheological properties, Yu et al. [13] proposed a dynamic torpedo-anchor technology. This technology mainly uses high-frequency mechanical vibrations to fluidize the sediment near the anchor body, thereby reducing the resistance between the outer wall of the anchor body and the surrounding soil so that the anchor body can automatically and quickly penetrate the seabed. When the anchor body penetrates the preset depth, the vibration unit is shut down and the installation is completed. The dynamic torpedo anchor has a large tensile-strength ratio and can withstand the vertical pullout force. It is characterized by fast anchor placement and easy recovery. Raaj et al. [14] stated that soil properties and shear strength affected the pullout capacity and penetration depth. Chen et al. [15] reported that the pullout capacity and penetration depth of the torpedo anchor with vibrational shearing was not restrained by water depth and drop height. Based on the embedment depth, net weight, geometry, and soil properties, Wang et al. [16] proposed a model to predict the undrained monotonic holding capacity of the torpedo anchor, and the predicted results coincided well with the experimental results. With increasing fin length, Ads et al. [17] concluded that the penetration depth decreased and the maximum extraction resistance increased. Kim and Hossain [18] stated that the inclined pullout capacity of torpedo anchors depended on the anchor weight and anchor-soil contact area; thereby, the pullout capacity increased with increasing fin number. Chen et al. [19] stated that the maximum vertical pullout capacity increased exponentially with increasing embedment depth under no vibrations, whereas the pullout capacity increased linearly with increasing embedment depth under 200 Hz vibrations. Hossain et al. [20,21] reported that the pullout capacity of the torpedo anchors increased with increasing consolidation time, embedment depth, and undrained shear strength, and the rectangular fin and conical tip were more effective to improve the pullout capacity. Based on the centrifuge model test results, an analytical model to calculate the pullout capacity of the torpedo anchor was established according to the reverse end-bearing and frictional resistance. Based on the nonlinear regression analysis of the test results, Wang et al. [22] established a model to predict the maximum inclined force of torpedo anchor penetration into cohesive beds when the loading angle changed from 20° to 90°. With increasing embedment depth, relative density, and area of the bearing plate, Li et al. [23] reported that the bearing capacity of the end-bearing torpedo anchor remarkably improved, and the pullout capacity of the end-bearing anchor was significantly higher than that of the traditional anchor. Yi et al. [24] found that the failure envelope was mainly influenced by anchor incline and soil strength gradient, and a simple procedure was developed to predict the ultimate pullout capacity of the torpedo anchor. Raie and Tassoulas [25] noted that the dissipation of excess pore water pressure and the recovery of soil strength were essential factors to predict the pullout capacity of the torpedo anchor.

Compared with the torpedo anchor without an anchor wing, the end-bearing torpedo anchor forms pile end resistance using a bearing plate, thus further improving its bearing capacity. However, there are fewer studies on the bearing capacity of end-bearing torpedo anchors. In this paper, we conduct the pullout model test of torpedo anchors without anchor wings and end-bearing torpedo anchors and analyze the bearing characteristics of both types of torpedo anchors under vertical and inclined pullout loads. Based on the test results, we establish the V-H envelope of the torpedo-anchor bearing capacity using the regression analysis method. The research findings can provide a reference for the optimization design and bearing-capacity prediction of torpedo anchors.

2. Materials and Methods

2.1. Test Materials

The test soil waswashed kaolin, purchased from Jiashuo Building Materials Processing Co., Ltd., Lingshou County, Shijiazhuang City, Hebei Province, China. According to the

standard for the geotechnical testing method (G/BT 50123-2019) [26], its basic physical properties are shown in Table 1.

Table 1. Main physical properties of kaolin.

G_s	ρ (g/cm^3)	w_L (%)	w_P (%)	I_P	S_u (kPa)	E (MPa)
2.60	1.60	42.3	21.3	21.0	1.63	0.82

The T-98 torpedo anchor wasselected as the model anchor. It is made of high-speed steel material, and its Young modulus and Poisson ratio was 200 GPa and 0.3, respectively. The anchor rod is 9.7 cm long, the anchor tip is 2.5 cm long, the anchor rod diameter (D) is 2 cm, and the anchor weighs 281.5 g. The anchor tip and the anchor rod are designed as two separate components, and the bearing plate can be assembled after detachment. A total of 12 types of bearing plates with a thickness of 2 mm were arranged for the test. The torpedo anchor without anchor wings (T type) is shown in Figure 1a, and the EN3 type torpedo-anchor bearing plate consists of 3 rectangular bearing plates with an angle of 120° for the center line, as shown in Figure 1b. The EN4-type torpedo-anchor bearing plate consists of 4 rectangular bearing plates with an angle of 90° for the center line, as shown in Figure 1c. The EC-type torpedo-anchor bearing plate was designed with a circular ring to ensure that the inner diameter of the bearing plate is the same as the outer diameter of the anchor rod and prevent the assembled bearing plate from any translation, as shown in Figure 1d. Table 2 lists the parameters of the torpedo-anchor bearing plate. As shown in the table, the size and weight of the rectangular bearing plate gradually increase with the increasing torpedo anchor number (1~4) when the type of bearing plate is fixed.

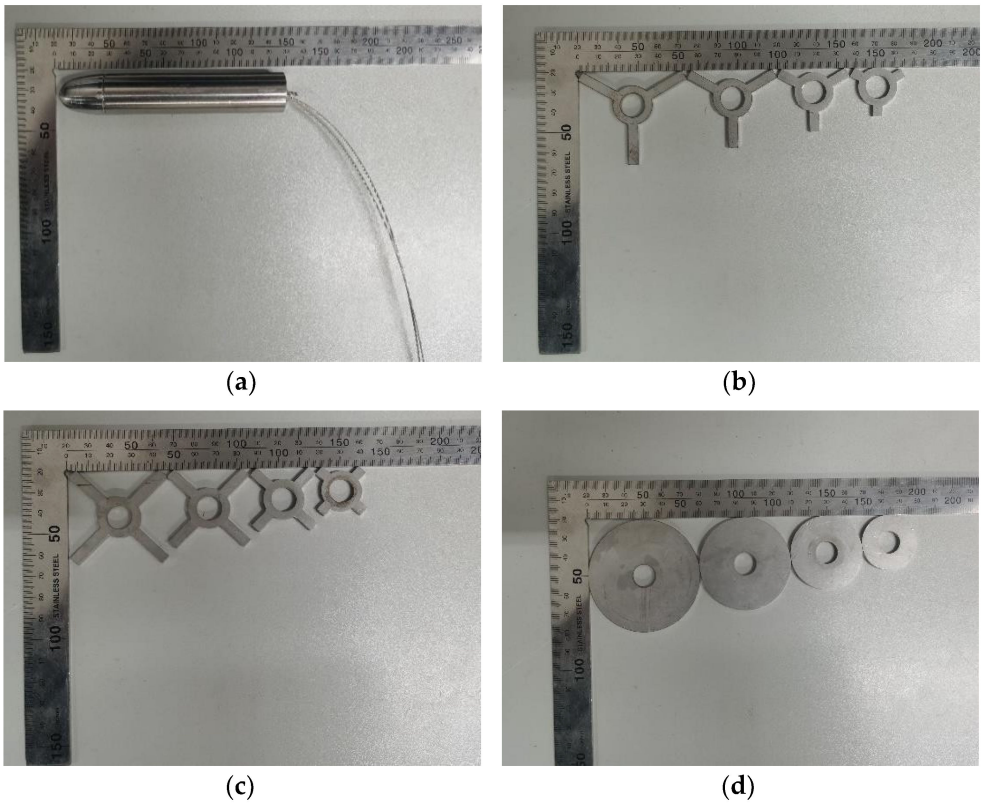

(**a**) (**b**) (**c**) (**d**)

Figure 1. Torpedo anchor and bearing plate: (**a**) torpedo anchor; (**b**) EN3 type; (**c**) EN4 Type; (**d**) EC type.

Table 2. Parameters of torpedo-anchor bearing plate.

Label	EN3 Type Dimensions (mm)	EN3 Type Mass (g)	EN4 Type Dimensions (mm)	EN4 Type Mass (g)	EC Type Diameter (mm)	EC Type Mass (g)
a	3 × 5 × 5	5.59	4 × 5 × 5	6.50	30	12.96
b	3 × 5 × 10	7.61	4 × 5 × 10	8.67	40	25.10
c	3 × 5 × 15	9.22	4 × 5 × 15	10.81	50	40.74
d	3 × 5 × 20	10.76	4 × 5 × 20	12.92	60	59.59

2.2. Test Equipment

The pullout test device is made of a rigid frame, as shown in Figure 2. It mainly consists of a fixed pulley, motor, tension sensor, signal amplifier, signal acquisition box, and computer. The steel strand connected to the motor side passes through the pulley fixed at the beam, the other end is connected to the top of the torpedo anchor, and the middle of the steel strand is connected to the type-S tension sensor. The sensor is connected to the signal amplifier through a data cable and outputs the signal to the TWD information acquisition box. The measuring range of the tension sensor is ±10 kg, the motor speed is 1 cm/s, and the acquisition frequency of the TWD information acquisition box is 200 Hz. The test model box is made of plexiglass, as shown in Figure 3. The height of the model box is 75 cm, the outer diameter is 45 cm, and the wall thickness is 2 cm. There are 6 holes in the outer wall of the model box. The lines connecting the center of the model box with the center of each hole form an angle of 0°, 15°, 30°, 45°, 60°, and 75° with the horizontal line, respectively, so that the torpedo can be pulled in multiple directions. When the soil sample is still and saturated, each hole is blocked with a rubber plug to prevent water leakage.

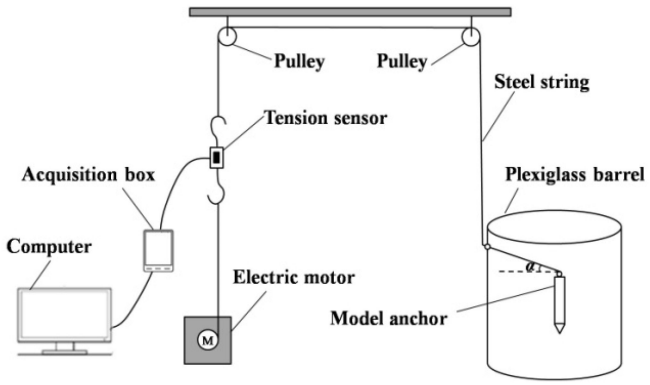

Figure 2. Schematic diagram of the model test device.

(**a**) (**b**) (**c**)

Figure 3. Flow chart of torpedo anchor installation: (**a**) installation; (**b**) vertically; (**c**) vibrating.

2.3. Test Methods

An amount of kaolin isslowly added into a proper amount of water, and we keep stirring to prevent kaolin from agglomerating and reduce bubble residues. Then, the model box is sealed with a plastic film to reduce soil moisture evaporation [23,26]. A steel strand

hole is reserved at the tail of the torpedo anchor in the test, two steel strands are inserted into the hole, and the steel strand and the torpedo anchor can be firmly connected by tightening the limit screw. The diameter of the steel strands is 2 mm, and the lengths are 44 cm and 137 cm, respectively. The steel strand with a constant length of 44 cm is used to ensure the same embedded depth of the torpedo anchor and the same height, with the pullout hole at 0° with the outer wall of the model box. A PVC pipe with a length of 37 cm, a wall thickness of 3 mm, and the same outer diameter as the outer diameter of the torpedo anchor is used as the conduit. Pass the steel strand through the conduit and press the conduit down to ensure that the bottom of the conduit fits the top of the anchor rod. Slowly press the torpedo anchor into the soil using the conduit. In this process, the torpedo moves down at a low constant speed to reduce the disturbance to the surrounding soil. See Figure 3 for the installation process. When the torpedo anchor reaches the embedded depth, a steel rod is placed on the surface of the model box to limit the downward movement of the torpedo anchor so that the anchor is successfully placed. Then, withdraw the conduit vertically and slowly to reduce the disturbance to the soil above and the impact on the torpedo anchor. Vibrate the soil around the hole wall at a high frequency but low amplitude to accelerate the soil body flow and complete the collapse of the soil above the anchor top. In the process of vibration, make sure that vibration points are symmetrical and far away from the hole locations to reduce the impact on the anchor position. When the torpedo anchor is installed, keep it still for 12 h to improve the soil strength, and set a thin water level on the soil surface in this process to prevent the soil from cracking. Then, remove the suspended steel rod and connect the steel strand with a length of 137 cm to the tension sensor and the motor. Adjust the fixed pulley position of the model box to make the steel strand pass through the middle of the hole, and apply Vaseline around the hole to reduce the test error. When performing the vertical pullout test, make sure that the steel strand above the top of the torpedo anchor is vertically upward. When performing the oblique pullout test, make sure that the steel strand is laid through the hole center by adjusting the fixed pulley at the outer wall so that the pullout angle of the steel strand meets the test requirements. Start the motor and stop the test when the load reaches the peak strength or the anchor body is fully pulled out. During the test, the data acquisition system is used to record the value and time of the tension sensor, and the load-displacement curve can be obtained after conversion according to the uniform speed pulling of the motor.

3. Results and Discussion

3.1. Results and Analysis of Vertical Pullout Test of Torpedo Anchor

Under the action of vertical pullout load, the bearing capacity of the torpedo anchor without an anchor wing is mainly provided by the side frictional resistance of the anchor rod, and the bearing plate of the end-bearing torpedo anchor has a significant effect on the bearing capacity improvement of the torpedo anchor. To study the effect of the bearing-plate length on the bearing capacity of an end-bearing torpedo anchor, Figure 4 shows the load-displacement relation curve of the EN3-type torpedo anchor. The figure shows that when the displacement is small, the load-displacement curve of the torpedo anchor increases in an approximately linear mode, and the curve fluctuates and tends to be stable with the increase of the displacement. As for the primary cause, it is believed that the soil around the anchor is in the stage of elastic deformation when the curve increases linearly and the soil enters the stage of plastic deformation at the inflection point of the curve. During the upward movement of the torpedo anchor affected by the pullout load, the upward movement of the anchor tip leads to the formation of a cavity in the original position and the generation of suction, so the load is reduced. Through the release of active soil pressure, the soil on the cavity side moves towards the cavity and the cavity is gradually filled, thus gradually reducing the suction and increasing the pullout load. The torpedo anchor moves upward at a constant speed. Therefore, cavities appear and are filled now and then, so the load-displacement curve fluctuates. Under the action of the vertical pullout load, the bearing plate has a significant effect on the bearing capacity

improvement of the torpedo anchor in comparison with the torpedo anchor without an anchor wing, and the bearing capacity rises with the increasing length of the bearing plate. When the length of the bearing plate is equal to the diameter of the anchor rod, the bearing capacity is increased by 0.78 times. When the length of the bearing plate is equal to the radius of the anchor rod, the bearing plate comes from the inside of the anchor rod more easily. Under such circumstances, the bearing capacity of the EN3-type torpedo anchor reaches 1.38 times that of the T-type torpedo anchor.

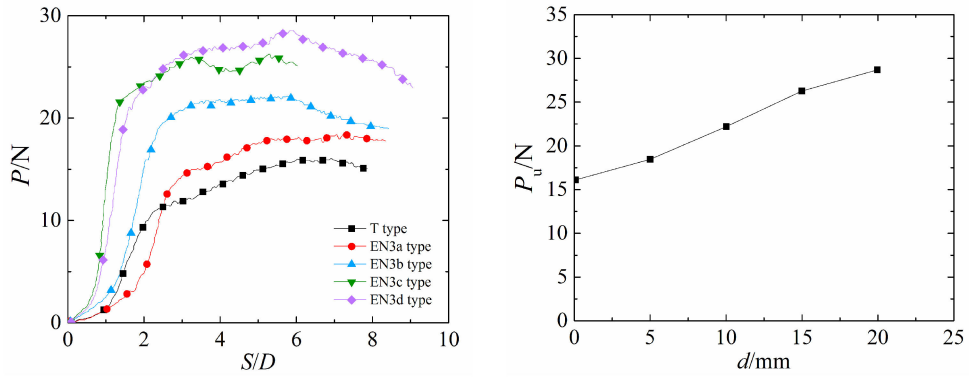

Figure 4. Relation curve between load and displacement of EN3-type torpedo anchor under vertical pullout load: (**a**) load-displacement curve; (**b**) bearing capacity–bearing-plate diameter curve.

Figure 5 shows the relation curve between the load and displacement of the EN4-type torpedo anchor. As shown in the figure, the findings are consistent with the previous study results. In detail, the bearing capacity of the torpedo anchor rises with the increasing length of the bearing plate and reaches the maximum value of 31.91 N when the length of the bearing plate is equal to the diameter of the torpedo anchor rod. The bearing capacity of the torpedo anchor is 24.59 N when the length of the bearing plate is equal to the radius of the torpedo anchor rod. In most cases, a longer bearing plate will provide a stronger bearing capacity. If the bearing plate is too long, it is difficult to install such a torpedo through structural design. Therefore, the length of the bearing plate involved in the test is limited to the range of 0.5 to 2 times the radius of the anchor rod. At the initial stage of pullout load for the torpedo anchor, the load increases linearly with the displacement. Under such circumstances, the soil is squeezed into the stage of elastic deformation by the anchor rod and the bearing plate, and the soil on the anchor side enters the stage of elastic deformation under the action of friction. However, the time nodes of entry into the stage of plastic deformation are not consistent. This finding is consistent with the conclusion of Richardson et al. [27].

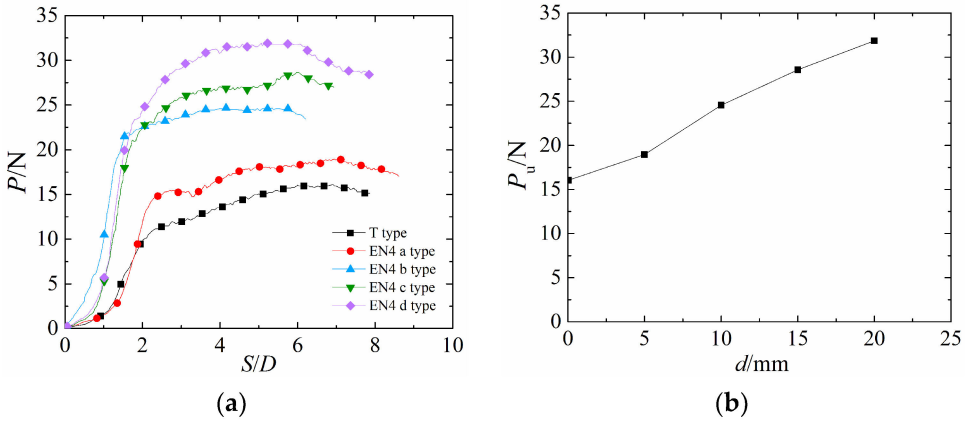

Figure 5. Relation curve between load and displacement of EN4-type torpedo anchor under vertical pullout load: (**a**) load-displacement curve; (**b**) bearing capacity–bearing-plate diameter curve.

In order to study the effect of the circular bearing-plate length on the bearing capacity of thetorpedo anchor, Figure 6 shows the load-displacement relation curve of the EC type of torpedo anchor. As shown in the figure, the bearing capacity of the torpedo anchor rises with the increasing radius of the bearing plate. When the radius of the bearing plate is equal to the diameter of the anchor rod, the bearing capacity of the end-bearing torpedo anchor is increased by 1.55 times compared with that of the torpedo anchor without the anchor wing. Figure 6b shows the relation curve between the bearing capacity and bearing plate radius of the EC torpedo anchor. As shown in the figure, a trend of approximate linear increase exists between the bearing capacity and the bearing-plate radius of the EC-type torpedo anchor, which is consistent with the above conclusion. When the bearing-plate radius is 20 mm, the bearing capacity of the torpedo anchor reaches 78.81 N, which ishigher than that of the T-type torpedo anchor. For the end-bearing torpedo anchor, the circular bearing plate forms a closed surface, which prevents the soil from flowing out of the bearing plate so that the bearing plate acts on the soil as a whole, further improving the bearing capacity. However, the circular bearing plate is an ideal type. In actual engineering practice, it is difficult for such a bearing plate to fully come from the anchor rod, while the EN3 and EN4 types of torpedo anchors can be constructed and installed more easily.

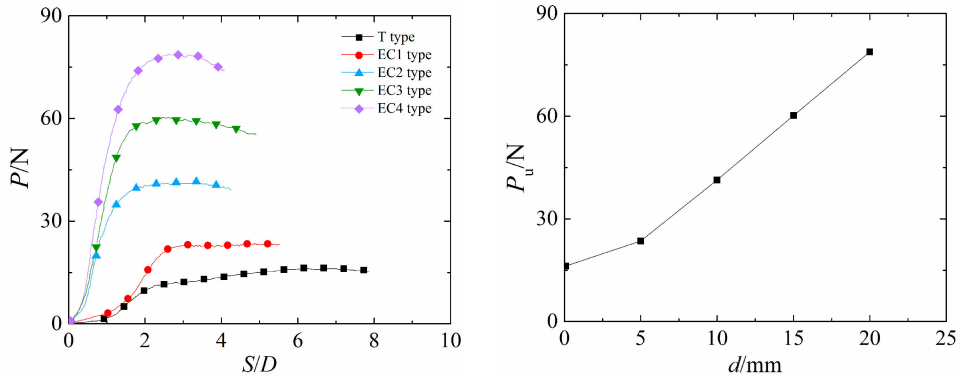

Figure 6. Relation curve between load and displacement of EC type torpedo anchor under vertical pullout load: (**a**) load-displacement curve; (**b**) bearing capacity–bearing-plate radius curve.

Figure 7 sums up the relation curves between the load and displacement of torpedo anchors with different types of bearing plates under vertical pullout load. As shown in the figure, the EC-type torpedo anchor can provide a greater bearing capacity than the EN3 and EN4 types of torpedo anchors, and the bearing-capacity difference gradually increases with the increasing length and diameter of the bearing plate. As for the primary cause, the EN3 and EN4 types of torpedo anchors have poor overall integrity with the increasing diameter of the bearing plate. Their bearing-capacity curve has a smaller slope than that of the EC-type torpedo anchors. The bearing plates of the EN3 and EN4 types oftorpedo anchors have the same effect on the bearing capacity of torpedo anchors, and the slope of the bearing-capacity curve of the EN4-type torpedo anchor is 1.23 times that of the EN3-type torpedo anchor, indicating that increasing the number and area of bearing plates can further improve the bearing capacity of torpedo anchors.

3.2. Results and Analysis of Inclined Pullout Test of Torpedo Anchor

Figure 8 shows the relation curve between the load, displacement, and pullout angle of a torpedo anchor without an anchor wing under an inclined pullout load. As shown in the figure, the bearing capacity of the torpedo anchor under an inclined pullout load is significantly increased compared with the bearing capacity under a vertical pullout load. The bearing capacity of the torpedo anchor without an anchor wing under different pullout angles is in the range of 18.25 N to 27.77 N and reaches the peak when the pullout angle is 45°. Based on comparisons, we discovered that the horizontal bearing capacity

of the torpedo anchor without an anchor wing is approximately 1.18 times the vertical bearing capacity.

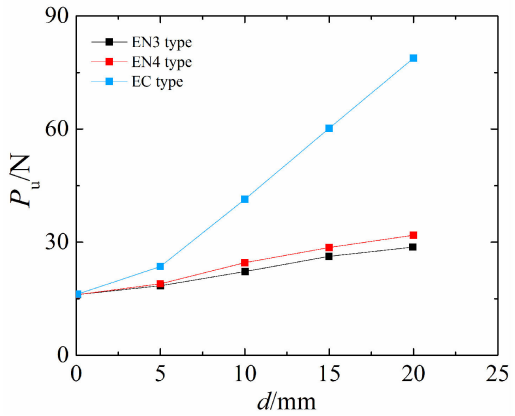

Figure 7. Relation curve between load and displacement of torpedo anchors with different types of bearing plates under vertical pullout load.

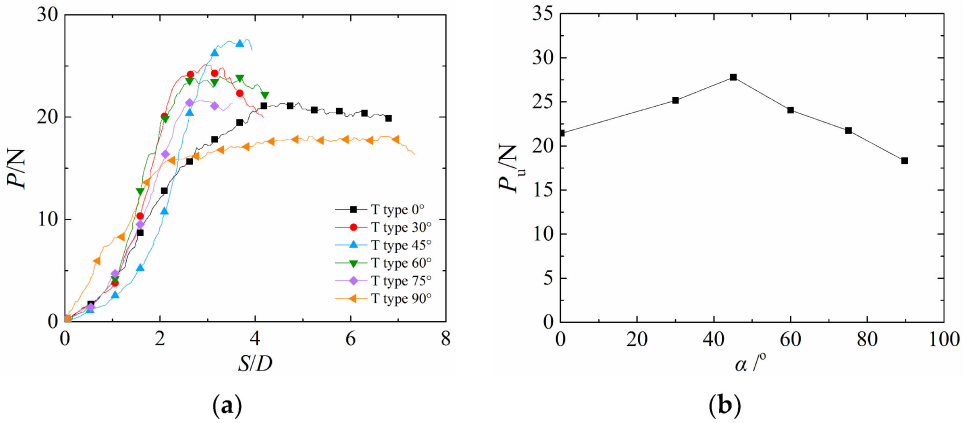

Figure 8. Relation curve between load, displacement, and pullout angle of T-type torpedo anchor under inclined pullout load: (**a**) load-displacement curve; (**b**) bearing capacity–pullout angle curve.

Figure 9 shows the relation curve between the load, displacement, and pullout angle of the EN3-type torpedo anchor under an inclined pullout load. As shown in the figure, the load-displacement curve of the torpedo anchor is approximately linear when there is a small displacement. Under such circumstances, it is believed that the soil around the anchor is in the stage of elastic deformation. When the pullout angle is in the range of 45° to 90°, the slope of the load-displacement curve is relatively large. When the pullout angle is 90°, the slope is the largest. Under the same test conditions, the horizontal bearing capacity of the EN3 torpedo anchor is 23.72 N, while the vertical bearing capacity is 21.86 N, indicating that the horizontal bearing capacity is 1.09 times the vertical bearing capacity. This fact is consistent with the research conclusion of O'Beirne [28]. For EN3-type torpedo anchors, the optimum pullout angle is 45°, and the corresponding bearing capacity is 28.03 N, which is about 1.28 times the vertical bearing capacity.

Figure 10 shows the relation curve between the load, displacement, and pullout angle of the EN4 torpedo anchor under an inclined pullout load. As shown in the figure, the load-displacement curve of the torpedo anchor under an inclined pullout load shows a trend of increasing first and then stabilizing. In the initial stage of load application, the curve increases in an approximately linear mode, and then the rate of increase gradually decreases and tends to be stable. When the torpedo anchor is subjected to vertical pullout, the anchor body moves from deep burial to shallow burial and then is gradually pulled out. Under such circumstances, the soil at the anchor top develops from local failure to

structural failure, and the resistance of the soil at the anchor top towards the torpedo anchor decreases gradually. The bearing capacity of the EN4-type torpedo anchor also shows the trend of increasing first and then decreasing with the increasing pullout angle, and the optimum pullout angle is 45°. Under such circumstances, the corresponding bearing capacity reaches the maximum value of 30.08 N.

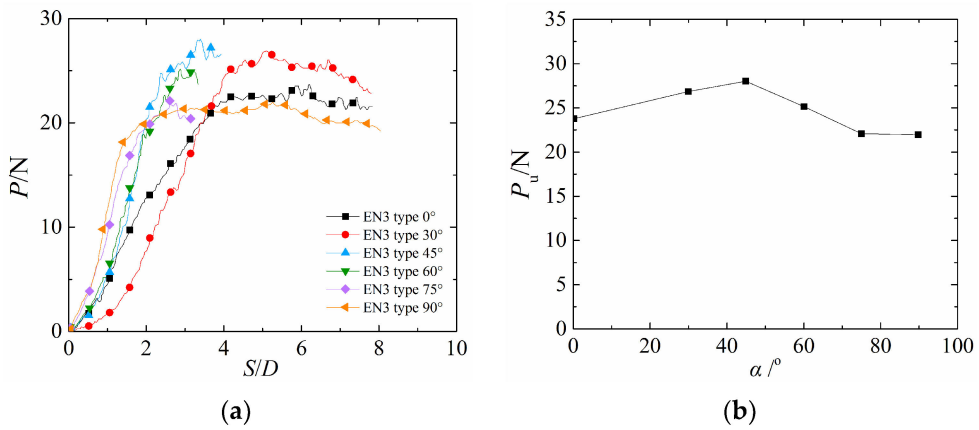

Figure 9. Relation curve between load, displacement, and pullout angle of EN3-type torpedo anchor under inclined pullout load: (**a**) load-displacement curve; (**b**) bearing capacity–pullout angle curve.

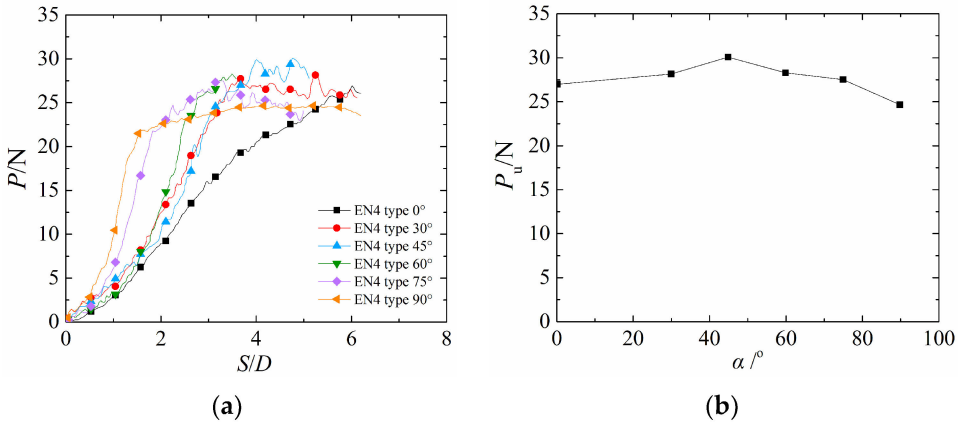

Figure 10. Relation curve between load, displacement, and pullout angle of EN4-type torpedo anchor under inclined pullout load: (**a**) load-displacement curve; (**b**) bearing capacity–pullout angle curve.

Figure 11 shows the relation curve between the load, displacement, and pullout angle of the EC-type torpedo anchor under an inclined pullout load. As shown in the figure, the torpedo anchor has the smallest bearing capacity under the vertical load. When the pullout angle is 45°, the bearing capacity reaches the peak. Under the vertical pullout load, the corresponding displacement is only 1 D when the bearing capacity reaches the peak. As for the primary cause, the bearing plate, anchor top, and soil around the anchor enter the stage of elastic deformation when the torpedo anchor is under vertical pullout. With the gradual increase of displacement, the soil evolves from the elastic stage to the critical plastic stage, and then the bearing capacity reaches the peak. When the displacement continues to increase, the bearing capacity will not increase. However, the soil deformation continues, which corresponds to the second half of the load-displacement curve, and the bearing capacity reaches a stable trend or gradual downward trend. When the torpedo anchor is subjected to a horizontal pullout load, a large displacement is required to make the bearing capacity reach the peak load. The torpedo anchor starts to rotate from the vertical position. When it reaches a certain angle, the torpedo anchor provides the maximum bearing capacity at thattime. In other words, the maximum bearing-capacity equivalent to that of horizontal

pullout is equivalent to the bearing capacity at a certain pullout angle. However, the peak horizontal bearing capacity is smaller than the peak bearing capacity at a specific angle mainly because the plastic deformation of the anchor top and anchor tip is the largest, and the plastic zone around the anchor expands with the rotation of the torpedo anchor when the torpedo anchor starts to rotate from the vertical position. When the torpedo anchor rotates to a certain angle, the soil around the anchor partially enters the stage of plastic deformation. Under such circumstances, the strength that the soil can provide is no longer the peak strength and maybe the residual strength. As shown in Figure 11, when the pullout angle changes from the vertical status to 45°, the bearing capacity of the torpedo anchor increases by 22.72% from 41.77 N to 51.26 N, indicating that the optimum pullout angle is 45°.

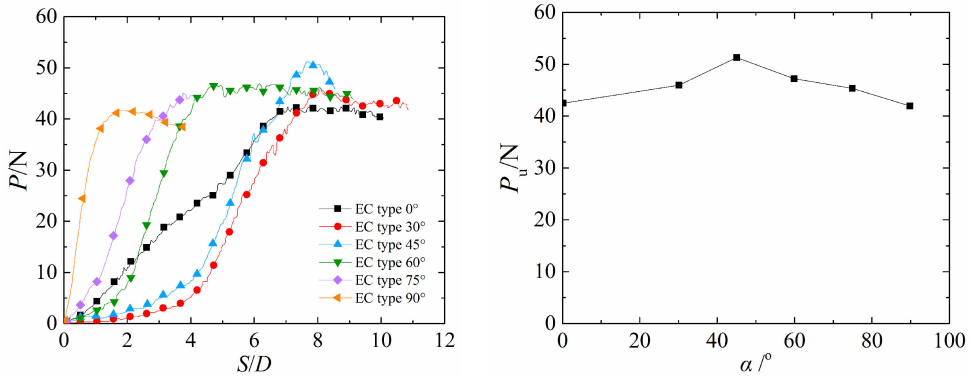

Figure 11. Relation curve between load, displacement, and pullout angle of EC-type torpedo anchor under inclined pullout load: (**a**) load-displacement curve; (**b**) bearing capacity–pullout angle curve.

Figure 12 sums up the relation curves between the bearing capacities of the T, EN3, EN4, and EC types of torpedo anchors and pullout angles. As shown in the figure, the bearing capacity of the torpedo anchors increases first and then decreases with the increasing pullout angle. When the pullout angle is 45°, the bearing capacity of all types of torpedo anchors reaches the peak. When the pullout angle is fixed, the bearing capacity of the T-typetorpedo anchor is the lowest, while the EC-type torpedo anchor has the largest bearing capacity, followed by the EN4-type torpedo anchor, indicating that the bearing capacity of the end-bearing torpedo anchor is significantly greater than that of the torpedo anchor without an anchor wing, and the bearing capacity of torpedo anchors rises with the increasing bearing-plate area.

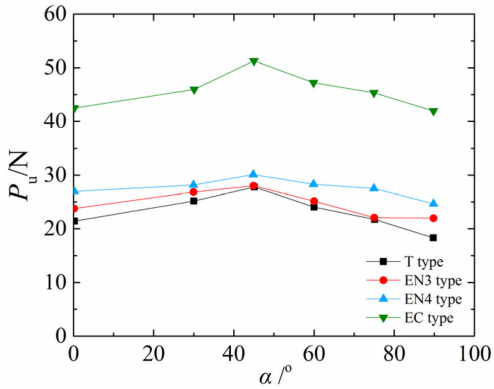

Figure 12. Relation curve between bearing capacity and pullout angle of torpedo anchor.

3.3. V-H Envelope Establishment

When studying the bearing capacity of torpedo anchors, the V-H bearing-capacity envelope is usually used to study the relations between the various components of bearing capacity [11]. The normalized V-H envelope is expressed as follows:

$$\left(\frac{P_{\mathrm{H}}}{P_{\mathrm{Hmax}}}\right)^{\mathrm{A}}+\left(\frac{P_{\mathrm{V}}}{P_{\mathrm{Vmax}}}\right)^{\mathrm{B}}=1 \tag{1}$$

where P_{H} is the horizontal component of the bearing capacity of the torpedo anchor; P_{V} is the vertical component of the bearing capacity of the torpedo anchor; P_{Hmax} is the maximum horizontal bearing capacity, also the bearing capacity during horizontal pullout; P_{Vmax} is the maximum vertical bearing capacity, also the bearing capacity during vertical pullout; and A and B are the envelope coefficients.

Based on the model test results and fitting analysis, we obtained the V-H failure envelope diagram of the bearing capacities generated by different types of torpedo anchors. See Figure 13 for details. Table 3 lists the bearing-capacity envelope coefficients of the torpedo anchors. As shown in the table, the determination coefficients of the EN3, EN4, and EC types of torpedo anchors are higher than 0.990, indicating a good correlation. In order to simplify the prediction of torpedo anchor bearing capacity, the unified regression analysis wascarried out on the test results of different types of torpedo anchors; the values of envelope coefficients A and B are 2.753 and 4.522, respectively, and the determination coefficient reaches 0.930, indicating that the formula is suitable for predicting the bearing capacity of different types of torpedo anchors. Different from classic elliptic stresses yield function [29,30], the V-H failure envelope was generated by the bearing capacities of different types of torpedo anchors. Due to the determination coefficients of the T-type torpedo anchor being only 0.553, the V-H failure envelope with hyperelliptic shape was formed.

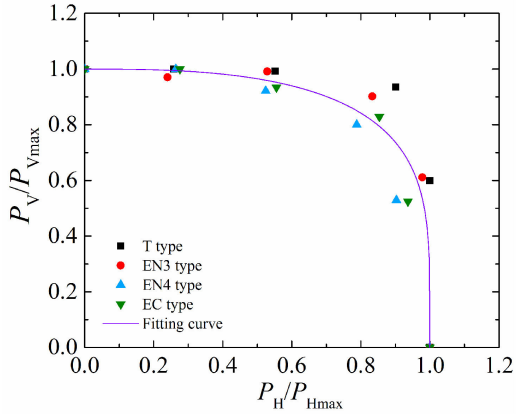

Figure 13. Bearing capacity V-H envelope.

Table 3. V-H envelope coefficient of bearing capacity.

Type	A	B	R^2
T	3.386	18.210	0.553
EN3	5.484	4.410	0.999
EN4	4.332	1.688	0.996
EC	10.484	1.090	0.995
Total	2.753	4.522	0.930

4. Conclusions

By conducting the pullout model test of torpedo anchors, we have studied the bearing characteristics of the T, EN3, EN4, and EC types of torpedo anchors under vertical loads and

inclined loads and compared and analyzed the effect of the pullout angle and bearing-plate radius on the bearing capacity of torpedo anchors. Based on the model test results, we established the V-H envelope of bearing capacity for different types of torpedo anchors. The findings of this study are of certain reference value for predicting the bearing capacity of torpedo anchors in engineering practice. The main conclusions are as follows:

(1) When the displacement is small under a vertical pullout load, the load-displacement curve of torpedo anchors shows the trend of approximately linear increase. The curve fluctuates and tends to be stable with the increase of the displacement. Compared with the torpedo anchor without an anchor wing, the bearing capacity of the end-bearing torpedo anchor is increased significantly and rises with the increasing bearing plate length. The EC-type torpedo anchor provides a greater bearing capacity than the EN3 and EN4 types of torpedo anchors.

(2) When the pullout angle is in the range of 0° to 45° under an inclined pullout load, the slope of the load-displacement curve of torpedo anchors is smaller. When the pullout angle is in the range of 45° to 90°, the slope of the load-displacement curve is larger. When the pullout angle is 90°, the curve has the largest slope.

(3) With anincreasing pullout angle, the bearing capacity of the torpedo anchor increases first and then decreases. When the pullout angle is 45°, the bearing capacity of all types of torpedo anchors reaches the peak. When the pullout angle is fixed, the bearing capacity of the T-type torpedo anchor is the lowest, while the EC-type torpedo anchor has the largest bearing capacity, indicating that the bearing capacity of an end-bearing torpedo anchor is significantly greater than that of a torpedo anchor without an anchor wing, and the bearing capacity of torpedo anchors rises steadily with the increasing bearing-plate radius or area.

(4) Based on the bearing capacity model test results of torpedo anchors, we established the V-H envelope of torpedo-anchor bearing capacity. Through regression analysis, it is concluded that for the torpedo anchors of T, EN3, EN4, and EC types, the envelope coefficients A and B of bearing capacity are 2.753 and 4.522 respectively, and the determination coefficient reaches 0.930, indicating that the established V-H envelope formula is suitable for predicting the bearing capacity of torpedo anchors.

Author Contributions: Conceptualization, J.Z. and G.L.; methodology, J.Z. and J.L.; validation, Y.X. and H.K.; writing—original draft preparation, J.L.; writing—review and editing, G.L.; funding acquisition, G.L. All authors have read and agreed to the published version of the manuscript.

Funding: This research was funded by the Natural Science Basic Research Program of Shaanxi Province, grant number 2021JM-535 and the Special Fund for Scientific Research by Xijing University, grant number XJ18T01.

Institutional Review Board Statement: Not applicable.

Informed Consent Statement: Not applicable.

Data Availability Statement: Not applicable.

Conflicts of Interest: The authors declare no conflict of interest.

References

1. Meng, K.; Cui, C.Y.; Liang, Z.M.; Li, H.J.; Pei, H.F. A new approach for longitudinal vibration of a large-diameter floating pipe pile in visco-elastic soil considering the three-dimensional wave effects. *Comput. Geotech.* **2020**, *128*, 103840. [CrossRef]
2. Cui, C.Y.; Zhang, S.P.; Chapman, D.; Meng, K. Dynamic impedance of a floating pile embedded in poro-visco-elastic soils subjected to vertical harmonic loads. *Geomech. Eng.* **2018**, *15*, 793–803.
3. Cui, C.Y.; Meng, K.; Wu, Y.J.; Chapman, D.; Liang, Z.M. Dynamic response of pipe pile embedded in layered visco-elastic media with radial inhomogeneity under vertical excitation. *Geomech. Eng.* **2018**, *16*, 609–618.
4. Cui, C.Y.; Liang, Z.M.; Xu, C.S.; Xin, Y.; Wang, B.L. Analytical solution for horizontal vibration of end-bearing single pile in radially heterogeneous saturated soil. *Appl. Math. Model.* **2023**, *116*, 65–83. [CrossRef]
5. Cui, C.Y.; Meng, K.; Xu, C.S.; Wang, B.L.; Xin, Y. Vertical vibration of a floating pile considering the incomplete bonding effect of the pile-soil interface. *Comput. Geotech.* **2022**, *150*, 104894. [CrossRef]

6. Cui, C.Y.; Xu, M.Z.; Xu, C.S.; Zhang, P.; Zhao, J.T. An ontology-based probabilistic framework for comprehensive seismic risk evaluation of subway stations by combining Monte Carlo simulation. *Tunn. Undergr. Space Technol.* **2023**, *135*, 105055. [CrossRef]
7. Cui, C.Y.; Meng, K.; Xu, C.S.; Liang, Z.M.; Li, H.J.; Pei, H.F. Analytical solution for longitudinal vibration of a floating pile in saturated porous media based on a fictitious saturated soil pile model. *Comput. Geotech.* **2021**, *131*, 103942. [CrossRef]
8. Dong, Y.K.; Wang, D.; Randolph, M.F. Investigation of impact forces on pipeline by submarine landslide using material point method. *Ocean Eng.* **2017**, *146*, 21–28. [CrossRef]
9. Dong, Y.K.; Cui, L.; Zhang, X. Multiple-GPU parallelization of three-dimensional material point method based on single-root complex. *Int. J. Numer. Meth. Eng.* **2022**, *123*, 1481–1504. [CrossRef]
10. Cheng, Y.; Qiu, C.L. Numerical analysis of torpedo anchor's uplift bearing capacity by material point method. *J. Waterw. Harb.* **2021**, *42*, 114–122.
11. Yu, L.; Zhang, J.L.; Yang, Q.; Yang, G. Capacity of torpedo anchor in clay using finite element analysis. *Ocean Eng.* **2019**, *37*, 122–129.
12. Yu, L.; Yang, Q.; Zhang, J.L.; Yang, G. Simplified model for upper bound method to analyze horizontal bearing capacity of torpedo anchors. *Chin. J. Geotech. Eng.* **2020**, *42*, 773–781.
13. Yu, G.L.; Wang, W.K.; Wang, C. The structure and characteristics of powered torpedo anchor. *Ocean Eng.* **2018**, *36*, 143–148.
14. Raaj, S.K.; Saha, N.; Sundaravadivelu, R. Exploration of deep-water torpedo anchors—A review. *Ocean Eng.* **2023**, *270*, 113607. [CrossRef]
15. Chen, X.H.; Zhang, M.X.; Yu, G.L. A self-penetration torpedo anchor with vibrational shearing. *Ocean Eng.* **2021**, *236*, 109315. [CrossRef]
16. Wang, W.K.; Wang, X.F.; Yu, G.L. Vertical holding capacity of torpedo anchors in underwater cohesive soils. *Ocean Eng.* **2018**, *161*, 291–307. [CrossRef]
17. Ads, A.; Iskander, M.; Bless, S.; Omidvar, M. Visualizing the effect of Fin length on torpedo anchor penetration and pullout using a transparent soil. *Ocean Eng.* **2020**, *216*, 108021. [CrossRef]
18. Kim, Y.H.; Hossain, M.S. Numerical study on pull-out capacity of torpedo anchors in clay. *Géotechnique Lett.* **2016**, *6*, 275–282. [CrossRef]
19. Chen, X.H.; Yu, G.L.; Yue, S.L.; Zhou, H. Effect of frequency of minute-amplitude oscillatory shear loadings on ultimate yield stress of cohesive sediments. *Appl. Ocean Res.* **2021**, *113*, 102542. [CrossRef]
20. Hossain, M.S.; Kim, Y.; Gaudin, C. Experimental Investigation of installation and pullout of dynamically penetrating anchors in clay and silt. *J. Geotech. Geoenviron. Eng.* **2014**, *140*, 04014026. [CrossRef]
21. Hossain, M.S.; O'Loughlin, C.D.; Kim, Y. Dynamic installation and monotonic pullout of a torpedo anchor in calcareous silt. *Geotechnique* **2015**, *65*, 77–90. [CrossRef]
22. Wang, C.; Chen, X.H.; Yu, G.L. Maximum force of inclined pullout of atorpedo anchor in cohesive beds. *China Ocean Eng.* **2019**, *33*, 333–343. [CrossRef]
23. Li, G.; Zhang, J.L.; Liu, J. Model test of the pullout bearing capacity of end-bearing torpedo anchors. *J. Mar. Sci. Eng.* **2022**, *10*, 728. [CrossRef]
24. Yi, J.T.; Fu, Y.; Liu, C.F.; Zhang, Y.H.; Li, Y.P.; Zhang, X.Y. Pull-out capacity of an inclined embedded torpedo anchor subjected to combined vertical and horizontal loading. *Comput. Geotech.* **2020**, *121*, 103478. [CrossRef]
25. Raie, M.S.; Tassoulas, J.L. Simulation of torpedo anchor set-up. *Mar. Struct.* **2016**, *49*, 138–147. [CrossRef]
26. *G/BT 50123-2019*; Standard for Geotechnical Testing Method. Construction Ministry of PRC: Beijing, China, 2019.
27. Richardson, M. Dynamically Installed Anchors for Floating Offshore Structures. Ph.D. Thesis, The University of Western Australia, Perth, Australia, 2008.
28. O'Beirne, C.; O'Loughlin, C.D.; Wang, D.; Gaudin, C. Capacity of dynamically installed anchors as assessed through field testing and three-dimensional large-deformation finite element analyses. *Can. Geotech. J.* **2015**, *52*, 548–562. [CrossRef]
29. Kavvadas, M.; Amorosi, A. A constitutive model for structured soils. *Geotechnique* **2000**, *50*, 263–273. [CrossRef]
30. Savvides, A.A.; Papadrakakis, M. A computational study on the uncertainty quantifcation of failure of clays with a modifed Cam-Clay yield criterion. *SN Appl. Sci.* **2021**, *3*, 659. [CrossRef]